

IGFBP2 and IGFBP4 interact to activate complement pathway in diabetic kidney disease

Jieling Liang^{a,b†}, Yangxiao Huang^{b†}, Daping Peng^b, Yali Xie^b, Yifei Liu^b, Xiuxia Lu^b and Junfa Xu^a

^aGuangdong Medical University, Dongguan, China; ^bDongkeng Hospital, Dongguan, China

ABSTRACT

Background: Diabetic kidney disease (DKD) is the leading cause of chronic kidney disease globally. Recent research has identified insulin-like growth factor-binding proteins 2 (IGFBP2) and 4 (IGFBP4) as potential biomarkers for DKD. Overactivation of the complement pathway in DKD remains poorly understood.

Methods: Blood samples were collected from patients for proteomic analysis, complemented by both *in vitro* and *in vivo* experiments to investigate the roles of IGFBP2, IGFBP4, and the complement pathway in DKD.

Results: Elevated levels of IGFBP2 and IGFBP4 were observed in DKD patients. The levels of IGFBP2 and IGFBP4 increased in DKD mice, accompanied by the activation of the complement pathway, and a deterioration in renal function. High glucose and serum from DKD mice stimulated an increase in the levels of IGFBP2 and IGFBP4 in HK-2 cells. The supernatant from HK-2 cells was used to culture THP-1 cells, resulted in an increase in the M1 type of THP-1 cells, a decrease in the M2 type, and activation of the complement pathway. The supernatant from THP-1 cells affected the growth of primary human renal podocytes. The exogenous addition of IGFBP2 and IGFBP4 proteins to primary human renal podocytes did not affect their growth. However, when human renal podocytes were cultured with the supernatant from THP-1 cells, the growth of the podocytes was affected.

Conclusions: IGFBP2 and IGFBP4 interact to stimulate the activation of the complement pathway in macrophages, which induces podocyte apoptosis and subsequently promotes the development of DKD.

ARTICLE HISTORY

Received 3 September 2024

Revised 20 November 2024

Accepted 5 December 2024

KEYWORDS



Diabetic kidney disease; IGFBP2; IGFBP4; complement pathway

Introduction

Diabetic kidney disease (DKD) represents a type of chronic kidney disease that develops as a complication of diabetes. The primary clinical signs of DKD include the presence of albumin in urine and (or) a glomerular filtration rate (GFR) below $60 \text{ mL} \cdot \text{min}^{-1} \cdot (1.73 \text{ m}^2)^{-1}$, lasting for over three months [1]. At present, DKD is responsible for nearly 50% of all chronic kidney disease cases worldwide. There is a critical necessity to improve both the diagnosis and management of DKD, enhance our understanding of the pathogenesis associated with DKD, and create more effective treatments that target the underlying mechanisms of DKD to help prevent its advancement.

Insulin-like growth factor binding proteins (IGFBPs) are a category of proteins that associate with insulin-like growth factor (IGF) ligands, modulating IGF's half-life in the bloodstream, its tissue distribution, and its interaction with cell

receptors [2]. Recently, there has been heightened interest in the significance of IGFBPs in relation to kidney diseases. The use of single-cell sequencing in adult kidneys has indicated that growth factor-binding proteins 2 (IGFBP2) is primarily expressed in podocytes, which play a crucial role in the development of DKD. Studies suggest that IGFBP2 may serve as an indicator of the progressive decline in renal function among individuals with type 2 diabetes, with an increase in IGFBP2 levels linked to a reduction in the estimated glomerular filtration rate (eGFR) and a rise in proteinuria [3]. Growth factor-binding proteins 4 (IGFBP4), recognized as the second most prevalent IGFBP in serum [4], shows extensive expression across a variety of tissues, including the liver, heart, brain, bone, ovary, muscle, prostate, and kidney [5]. Importantly, the notable rise of Angiotensin Like 8 (ANGPTL8), identified as a recognized risk factor for DKD in those with type 2 diabetes, is closely associated with IGFBP4. This implies that IGFBP4 might be significantly involved in

CONTACT Junfa Xu  xujunfa@gdmu.edu.cn  Guangdong Medical University, Dongguan, Guangdong 523808, China

[†]Co-author.

© 2025 The Author(s). Published by Informa UK Limited, trading as Taylor & Francis Group

This is an Open Access article distributed under the terms of the Creative Commons Attribution-NonCommercial License (<http://creativecommons.org/licenses/by-nc/4.0/>), which permits unrestricted non-commercial use, distribution, and reproduction in any medium, provided the original work is properly cited. The terms on which this article has been published allow the posting of the Accepted Manuscript in a repository by the author(s) or with their consent.

the pathophysiological processes of DKD and could potentially act as a valuable diagnostic marker for its identification [6]. Nonetheless, additional studies are necessary to clarify the biological roles of IGFBP2 and IGFBP4 in DKD, their possible interconnections, and the mechanisms by which they contribute to the disease's progression.

The complement system plays a vital role as an effector in the innate immune response [7]. Nevertheless, excessive activation of this system has been associated with various immune-mediated kidney disorders [8], including atypical hemolytic uremic syndrome (aHUS), C3 glomerular disease, IgA nephropathy (IgAN), lupus nephritis (LN), and rejection of renal transplants [9]. Complement component 3a (C3a) and complement component 5a (C5a) function as the main effector molecules within the complement cascade. Importantly, complement deposition has been identified in the kidneys of individuals suffering from DKD, where elevated C5a levels were noted in the renal tubules. Moreover, the degree of C5a staining exhibited a positive correlation with the advancement of renal disease in these patients. A comparative analysis of the transcriptomes from matched control samples of kidney patients experiencing early DKD and non-diabetic subjects indicated that alterations in the complement pathway were the most pronounced. In particular, the complement component 7 (C7) gene expression in both serum and kidney tissue of DKD patients showed a twofold increase [10].

This study identifies a protein interaction relationship between IGFBP2 and IGFBP4, two key proteins implicated in the development of DKD, through proteomic analysis. Functional enrichment analysis revealed that both IGFBP2 and IGFBP4 are associated with the complement pathway. Furthermore, the proteomic findings were corroborated by both *in vivo* and *in vitro* experiments. These results suggest that the interaction between IGFBP2 and IGFBP4 activates the complement pathway in macrophages, leading to further damage to podocytes and promoting the progression of DKD. This work offers a novel strategy for the prevention and treatment of DKD.

Materials and methods

Clinical sample collection

The inclusion criteria for patients with DKD are as follows: fasting blood glucose levels must be ≥ 7.0 mmol/L (126 mg/dL) on two consecutive occasions. Additionally, the patient must exhibit elevated urine protein levels, indicated by a urinary albumin-to-creatinine ratio of ≥ 30 mg/g, and/or a GFR < 60 mL \cdot min $^{-1}\cdot(1.73$ m $^2)^{-1}$, which must persist for more than three months. Other potential causes must also be excluded. The inclusion criteria for patients with diabetes are as follows: fasting plasma glucose levels of ≥ 130 mg/dL, and/or a 2-h plasma glucose (2hPG) level of ≥ 200 mg/dL, and/or three points on the oral glucose tolerance test (OGTT) curve that exceed the diagnostic thresholds (with the 0-min value at 125 mg/dL, 60 min at 180 mg/dL, 120 min at 140 mg/dL, and 180 min at 125 mg/dL). Blood samples were collected from 23 patients with DKD, nine diabetic patients, and 11 normal

controls for subsequent proteomic analysis and verification of the results. This study protocol of experiments on humans was reviewed and approved by Ethics Committees of Dongkeng Hospital. All methods were carried out in accordance with relevant guidelines and regulations. Verbal informed consent was obtained from all subjects and was in line with local guidelines.

Experimental animal

All mice were obtained from the Guangdong Medical Laboratory Animal Center (<https://gdmlac.com.cn/>). Six-week-old male C57BL/6J mice weighing 20 ± 2 g were randomly assigned to two groups: the normal control group (CK) and the DKD group (DK), with 10 mice in each group, following a 1-week acclimatization period. The CK group received a standard diet, while the DK group was administered a high-fat diet comprising 60% of total caloric intake. After 4 weeks, the DK group underwent intraperitoneal injection of a low dose of streptozotocin (STZ) at 30 mg \cdot kg $^{-1}$ for 1 week, whereas the CK group received an equivalent volume of sodium citrate buffer. Following a 1-week period post-STZ injection, fasting blood glucose levels were monitored, with mice exhibiting blood glucose levels exceeding 13.8 mM classified as successfully modeled. Upon confirmation of successful modeling, the CK group continued on the normal diet, while the DK group maintained the high-fat diet. Urine samples were subsequently collected from the mice. Subsequently, the mice were euthanized through inhalation of excess carbon dioxide, and plasma and kidney tissue samples were collected post-euthanasia for further analysis. The study protocol of animal experiments was reviewed and approved by the Institutional Animal Care and Use Committee (IACUC) of Ruige Biotechnology (Ningbo, China), approval number (20240508-002) and the animal experiments were performed in the accordance with Animal Research: Reporting of In Vivo Experiments (ARRIVE) guidelines (<https://arriveguidelines.org>).

Proteomic analysis

After quantifying the plasma samples, an equal volume from each sample is pooled to create a single sample for the generation of Data Independent Acquisition (DIA) database and subsequent quality control. Each sample is then transferred to a filter to collect the peptides present in the filtrate. An indexed Retention Time (iRT) calibration peptide is added to the pooled sample, which is subsequently fractionated into 10 distinct fractions. All fractions undergo analysis using mass spectrometers and chromatographic systems from Thermo Fisher Scientific (Waltham, MA). Protein databases are downloaded from NCBI (RefSeq) and UniProt for further analysis. Clustering analysis is performed to assess differences in protein expression, alongside protein interaction network analysis. Additionally, Gene Ontology (GO) analysis (<http://geneontology.org/>) and Kyoto Encyclopedia of Genes and Genomes (KEGG) analysis (<https://www.genome.jp/kegg/>) are conducted.

Insulin tolerance test (ITT)

Mice were fasted for 6 h. A drop of blood was taken from the tip of the mouse's tail, and blood glucose levels were measured using a blood glucose meter. The recorded value represents the blood sugar level at 0 min. After allowing the mice to acclimate for 10 min, an insulin solution ($0.01 \text{ mL}\cdot\text{g}^{-1}$) was injected intraperitoneally, with a 1-min interval between each mouse's procedure. Blood glucose levels for each mouse were measured at 15, 30, 60, 90, and 120 min following the injection.

Enzyme-linked immunosorbent assay (ELISA)

Standard and sample wells were established. A detection antibody labeled with horseradish peroxidase (HRP) was added at a volume of $100 \mu\text{L}$ to each well, followed by incubation in a water bath at 37°C for 60 min. Subsequently, $50 \mu\text{L}$ of substrate was added to each well, and the wells were incubated at 37°C for 15 min in the dark. Finally, $50 \mu\text{L}$ of termination solution was added, and the optical density (OD) values of each well were measured at a wavelength of 450 nm.

Hematoxylin-eosin (HE) staining

The tissue slices were treated with xylene for 10 min, followed by a dewaxing process. Subsequently, they were immersed in a hematoxylin solution for 5 min, after which excess dye was removed under running water. The sections were differentiated using 1% hydrochloric acid alcohol for 10 s and then rinsed again under running water. To reverse the blue coloration, the sections were treated with 0.6% ammonia and rinsed once more under running water. Following this, the sections, now exhibiting a blue hue, were immersed in eosin dye for 5 min, with any excess dye eluted using running water. After staining, the sections underwent gradient dehydration before being immersed in xylene for 5 min to achieve transparency. Finally, the sections were sealed with neutral gum and observed using the Mshot digital imaging system (Guangzhou, China).

Periodic acid-Schiff (PAS) staining

The sections were dewaxed in water and subsequently treated with prepared periodate alcohol for 10 min. Following this, they were rinsed with water and stained with Schiff's solution for an additional 10 min to achieve complete cytoplasmic staining. The sections were then stained with hematoxylin for 3 min to finalize the staining of the cell nuclei. After rinsing with running water, the sections underwent routine dehydration, transparency treatment, and sealing, before being observed under the microdigital imaging system of Mingmei (Guangzhou, China).

Masson staining

The sections were dewaxed and stained using Weigert's iron hematoxylin solution for 8 min, followed by differentiation

with an acid ethanol solution for 15 s. Subsequently, the sections were treated with Masson blue solution for 5 min, rinsed in distilled water for 1 min, and stained with ponceau-fuchsin dyeing solution for 5 min. This was followed by treatment with a weak acid working solution for 1 min, phosphomolybdic acid solution for 1 min, and another application of the weak acid working solution for 1 min. The sections were then stained with aniline blue dyeing solution for 2 min, followed by weak acid pickling for 1 min to complete the staining process. After staining, gradient dehydration was performed, and xylene transparency was achieved through three rounds of cutting sections, which were then sealed with neutral resin and observed using the microdigital imaging system from Mingmei (Guangzhou, China).

Western blot (WB)

Total protein was extracted and centrifuged at high speed at 4°C . The supernatant was collected and subjected to protein electrophoresis using a 10% SDS-PAGE gel under a constant voltage of 120 V. Following this, the supernatant was transferred at 75 V for 90 min after a 1-h incubation, sealed with 5% normal calf serum for 1 h, and subsequently washed three times with TBST buffer. Primary antibodies were then added, including IGFBP4 (PA5-25925, Thermo Fisher, Waltham, MA), IGFBP2 (PA5-79450, Thermo Fisher, Waltham, MA), C3 (PA5-21349, Thermo Fisher, Waltham, MA), C4B (22233-1-AP, Proteintech, Wuhan, China), C5 (ab275931, Abcam, Cambridge, UK), C9 (ab168345, Abcam, Cambridge, UK), GAPDH (ab8245, Abcam, Cambridge, UK), and transferrin (PA5-27306, Thermo Fisher, Waltham, MA). These were incubated overnight at 4°C , followed by washing with TBST buffer. The samples were then combined with Goat Anti-Mouse IgG/HRP (SE131, Solarbio, Beijing, China) and Goat Anti-Rabbit IgG H&L (HRP) (ab6721, Abcam, Cambridge, UK), and incubated at room temperature for 2 h. ECL color development was performed, and gray values were measured using an automatic gel imaging analyzer.

Immunohistochemistry

Renal tissue was fixed in 4% paraformaldehyde and subjected to a series of gradient dehydration steps, followed by sectioning, dewaxing, and gradient hydration. A solution containing 3% BSA was prepared and sealed at room temperature for 30 min. After drying the sealing liquid, the primary antibodies (IGFBP4: PA5-25925, Thermo Fisher, Waltham, MA; IGFBP2: PA5-79450, Thermo Fisher, Waltham, MA; complement component 3 (C3): PA5-21349, Thermo Fisher, Waltham, MA; complement component 4B (C4B): 22233-1-AP, Proteintech, Wuhan, China; complement component 5 (C5): ab275931, Abcam, Cambridge, UK; complement component 9 (C9): ab168345, Abcam, Cambridge, UK) were added and incubated in a wet box at 4°C overnight. Following incubation, the samples were washed with shaking, and corresponding secondary antibodies (Goat Anti-Mouse IgG/HRP: SE131, Solarbio, Beijing, China; Goat Anti-Rabbit IgG H&L

(HRP): ab6721, Abcam, Cambridge, UK) were added and incubated at room temperature for 50 min. The samples were then washed in PBS with shaking, followed by the addition of DAB color developing solution. After rinsing the slices with tap water to halt color development, hematoxylin was applied for approximately 3 min to re-stain, and ammonia water was used to restore the blue color. The samples underwent gradient dehydration and were sealed with neutral gum before microscopic images were captured using the Mingmei digital imaging system (Guangzhou, China).

Cell culture

Human embryonic kidney cell 293T (CRL-3216, ATCC, Manassas, VA), human tubular epithelial cell HK-2 (CRL-2190, ATCC, Manassas, VA), and macrophage THP-1 (TIB-202, ATCC, Manassas, VA) were obtained and certified by ATCC (<https://www.atcc.org/>). The primary human renal podocytes were purchased from Wuhan Punosay Life Technology Co., Ltd. (CP-H075) (Wuhan, China). 293T cells and primary human renal podocytes were inoculated and grown in DMEM high-glucose medium, HK-2 cells were inoculated and grown in DMEM/F-12 medium, and THP-1 cells were inoculated and grown in 1640 medium with 10% fetal bovine serum, 1% 100 µg/mL penicillin and streptomycin. The cells were cultured in a 5% CO₂ incubator at 37°C.

Quantitative real-time PCR (qPCR)

Cells were lysed using Trizol solution, and RNA was extracted with chloroform and isopropyl alcohol. Reverse transcription of mRNA was conducted following the M5 First Strand cDNA Synthesis Kit protocol from Jumei Company (Beijing, China), and subsequent RT-qPCR was performed on the cDNA obtained from this reverse transcription. The experimental procedure adhered to the method outlined in the PerfectStart™ Green qPCR SuperMix kit. The primer sequences used were as follows: GAPDH (AATGACCCCTTCATTGAC, TCCACGACGACTCAGCGC), IGFBP4 (GGACTCAGTGCCCC TACTA, CCTACCCCATTCCTTCCC), and IGFBP2 (AAGCATGC GGCGTCTACATC, GTCATCACTGTCTGCAACCTG).

Overexpression of IGFBP2

The IGFBP2 gene sequence was synthesized by Beijing Qingke Biotechnology Co., Ltd. (Beijing, China). The successful construction of the overexpressed IGFBP2 plasmid was confirmed through qPCR and WB analysis. Twenty hours post-transfection, the 293T cells were replenished with fresh medium and continued to be cultured. After 48 h, the supernatant from the cell culture was collected. Subsequently, 293T cells were plated in 24-well plates and cultured overnight before being infected with lentivirus. Twenty-four hours after infection, the culture medium containing the virus was discarded and replaced with fresh complete culture medium, allowing for continued culture. After another 48 h, the

medium was replaced with fresh complete culture solution containing puromycin to select for stable transduced cell lines.

Co-immunoprecipitation (Co-IP) assay

Each cell pore plate was treated with 150 µL of inhibitor-containing lysate. Following complete lysis, the supernatant was obtained by centrifugation at 12,000 × *g* for 5 min at 4°C. The prepared protein A + G magnetic beads were magnetically separated, and the supernatant was discarded. Subsequently, 500 µL of antibody working solution at a concentration of 25 µg·mL⁻¹ was added, and the mixture was incubated at room temperature for 30 min with gentle suspension. After incubation, 500 µL of TBS was added, and the sample was placed on a magnetic rack for 10 s to remove the supernatant. This washing step was repeated three times. For each 500 µL protein sample, 20 µL of magnetic bead suspension was added and incubated at 4°C overnight. After incubation, the sample was separated on a magnetic rack for 10 s to discard the supernatant. Following this, 0.5 mL of inhibitor-containing lysate was added, and separation was performed for 10 s, after which the supernatant was removed. The washing with inhibitor-containing lysate was repeated three times. Finally, 100 µL of loading buffer (1×) was added to each 20 µL of magnetic beads, and the mixture was heated at 95°C for 5 min. After heating, the sample was placed on a magnetic rack for 10 s, and the supernatant was collected for subsequent WB detection.

Flow cytometry

Induced macrophages were collected and identified through flow cytometry utilizing fluorescence-labeled antibodies against cluster of differentiation 86 (CD86) and cluster of differentiation 206 (CD206). The rates of apoptosis were assessed using the ANNEXIN V-FITC/PI apoptosis detection kit (Solarbio, Beijing, China) via flow cytometry.

Cell counting kit-8 (CCK-8)

A total of 10 µL of CCK8 solution was added to each well of a 96-well plate, followed by a 2-h incubation period. The absorbance at 450 nm was measured using an enzyme-labeled instrument. The cell survival rate was calculated using the formula: cell survival rate (%) = [(As - Ab)/(Ac - Ab)] × 100, where As represents the absorbance of the experimental well, Ab denotes the absorbance of the blank well, and Ac indicates the absorbance of the control well.

Reactive oxygen species (ROS) detection

ROS content was quantified using a Reactive Oxygen Species Assay Kit (Beyotime, China). Following the loading of the probe, 2 mL of DCFH-DA at a final concentration of 10 µmol·L⁻¹ was added and incubated in a cell incubator at 37°C for

20 min. The cells were then washed three times. The expression of ROS in the cells was directly observed using a fluorescence microscope.

Statistical analysis

All the data are presented as the mean \pm SD, and group differences were determined via one-way analysis of variance (ANOVA). GraphPad Prism 9.0 (GraphPad Software, Inc., La Jolla, CA) was used for statistical analyses with $p < .05$ considered statistically significant.

Results

The expression of IGFBP2 and IGFBP4 was increased in DKD patients

To investigate the key proteins involved in DKD, we collected plasma samples from normal adults, diabetic patients, and those with DKD for proteomic analysis. Our findings revealed that 29 proteins were exclusively expressed in patients with DKD, while 68 proteins were co-expressed in both diabetic and DKD patients (Figure 1(A)). A heat map analysis was conducted (Figure 1(B)), revealing that the expression levels of eight proteins were significantly different from those in the normal group (Figure 1(C)). Network interaction analysis indicated that filamin A (FLNA) (P21333 protein) among the differentially expressed proteins interacted with cadherin 1 (CDH1) and melanoma cell adhesion molecule (MCAM). Notably, within the subset of specific proteins associated with the DKD group, we observed an interplay between IGFBP2 (P10646 protein) and IGFBP4 (A1508 protein), as well as between tissue factor pathway inhibitor (TFPI) (P18065 protein) and serine protease 3 (PRSS3) (A024R1U8 protein) (Figure 1(D,E)). Additionally, through GO and KEGG enrichment analyses, we established that the specific proteins associated with DKD are linked to the complement pathway (Figure 1(F,G)). The detection of IGFBP2 and IGFBP4 levels in plasma revealed an increase in the protein expression of both IGFBP2 and IGFBP4, suggesting that these proteins may promote the development of DKD (Figure 1(H)).

IGFBP2 and IGFBP4 promote the development of DKD in mice

In DKD mice, blood albumin levels significantly decreased from week 5 to week 6, while fasting blood glucose levels rose markedly from week 3 to week 6. Additionally, serum creatinine levels exhibited a significant increase from week 3 to week 6 (Figure 2(A)). ITT was conducted in the sixth week, and the results indicated that, compared to the CK group, the blood glucose concentration in the DK group increased, along with an increase in the area under the curve (AUC), suggesting a rise in insulin resistance (Figure 2(B)). Furthermore, renal function indicators demonstrated that both urinary albumin and urinary creatinine levels significantly increased from week 3 to week 6, with urinary sugar

levels also showing a significant increase from week 2 to week 6 (Figure 2(C)). Histological examination through HE staining indicated an increase in glomerular volume in DKD mice, accompanied by renal tubular dilation and a degree of inflammatory infiltration. PAS staining corroborated these findings, showing increased glomerular volume, thickening of the basement membrane, and substantial glycogen deposition in the DK group. Masson's staining revealed significant collagen accumulation in both the glomeruli and the tubulointerstitial of DKD mice (Figure 2(D)). Concurrently, we observed that the expressions of IGFBP2 and IGFBP4 in the plasma of DKD mice significantly increased from week 3 to week 6 (Figure 2(E)), showing a positive correlation with fasting blood glucose and blood muscle levels, while demonstrating a negative correlation with blood albumin levels (Figure 2(F)).

IGFBP2 and IGFBP4 interact to activate the complement pathway in DKD mice

Enrichment analysis of clinical samples indicated a relationship between IGFBP2 and IGFBP4 proteins and the complement pathway. Consequently, we examined the alterations in the levels of IGFBP2, IGFBP4, and complement proteins in the plasma and kidney tissue of mice with DKD. Our findings revealed that the expression of IGFBP2 and IGFBP4 proteins was significantly elevated in both plasma and kidney tissues of these DKD mice. This increase was accompanied by elevated levels of complement proteins C3, C4B, C5, and C9 (Figure 3(A–C)), as well as a significant rise in the membrane attack complex (MAC) resulting from the complement pathway in the plasma of DKD mice. In contrast, no significant changes were observed in the plasma levels of mannose-binding lectin (MBL) from the MBL pathway (Figure 3(D)). To further validate our findings, 293T cells were utilized to confirm the results of the protein network interaction analysis. Following the overexpression of IGFBP2 in 293T cells, we noted a significant increase in the expression levels of both IGFBP2 and IGFBP4 (Figure 4(A,B)). Subsequently, we conducted a Co-IP assay to determine whether IGFBP2 can bind to IGFBP4. The results demonstrated that either IGFBP2 or IGFBP4 protein could successfully pull down the other, indicating that IGFBP2 and IGFBP4 interact and form a complex (Figure 4(C)).

The crosstalk effect of HK-2 cells, THP-1 cells, and primary human renal podocytes

To investigate the crosstalk effect of HK-2 cells, THP-1 cells, and primary human renal podocytes, the serum from DKD mice (10%) or a high-glucose medium was added to HK-2 cells for culture for 24 h, after which relevant indicators were detected. The supernatant from HK-2 cells was then transferred to THP-1 cells for 24 h to assess the functional changes in THP-1 cells, and subsequently, the serum from DKD mice (10%), a high-glucose medium or the THP-1 cell supernatant was added to primary human renal podocytes

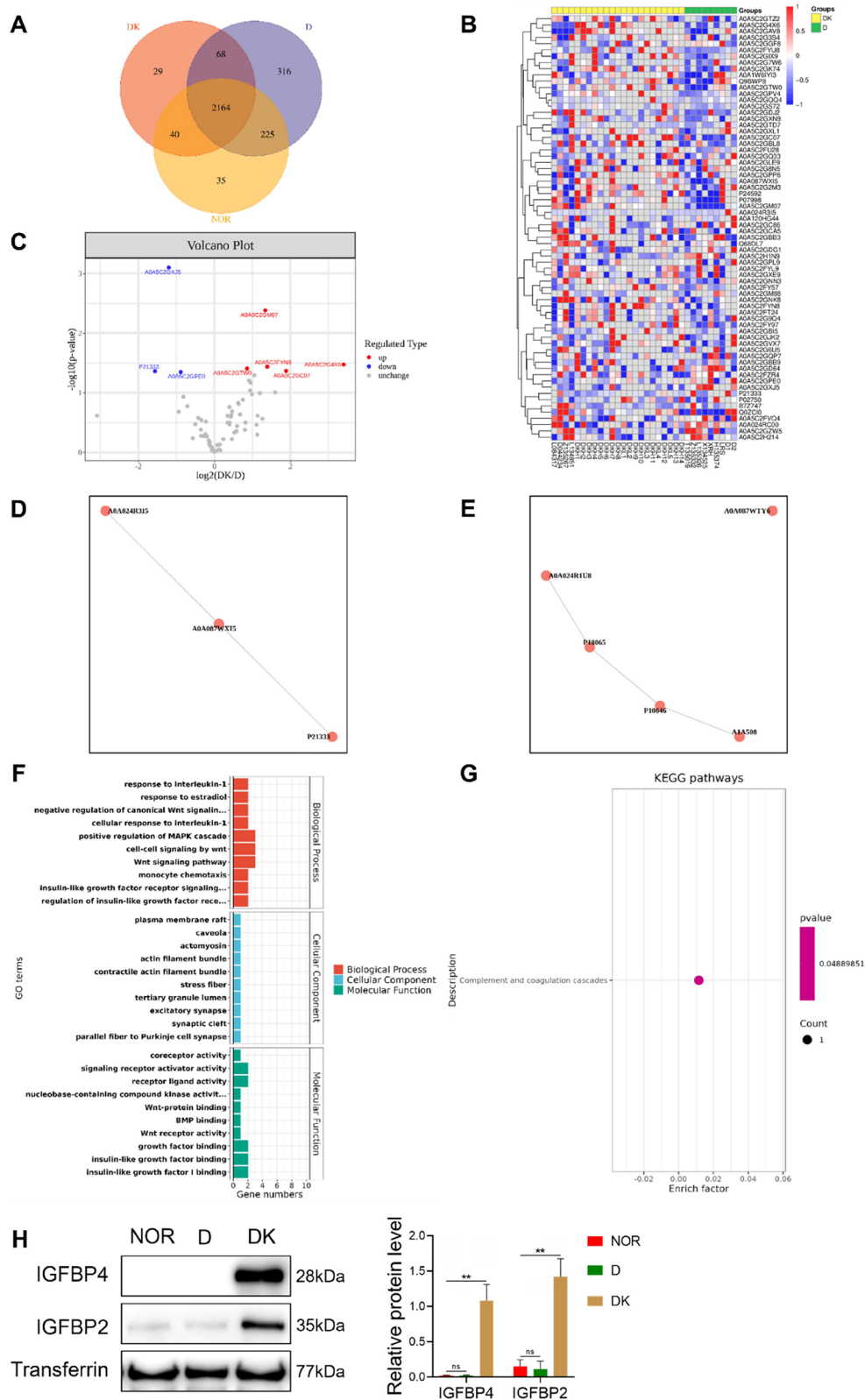
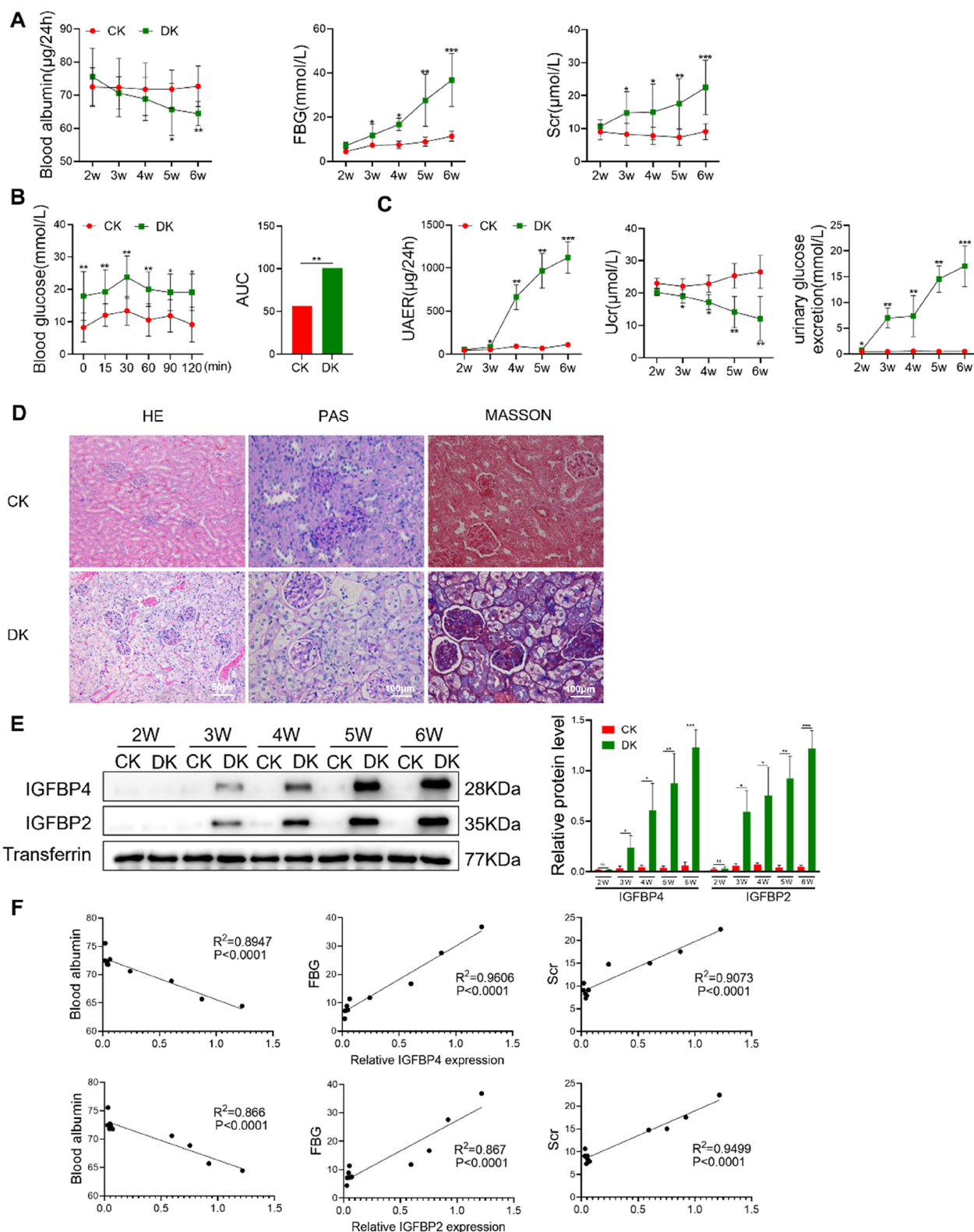


Figure 1. The proteomic analysis of plasma was conducted across three groups: normal adults, diabetic patients, and patients with diabetic kidney disease. (A) A Venn diagram was utilized to analyze the sequenced proteins, where group D represents the plasma samples from diabetic patients, group DK denotes the plasma from DKD patients, and group nor corresponds to the plasma of normal adults. The numbers indicate the count of sequenced and annotated proteins. (B) Heat maps were generated to analyze the differential expression of plasma proteins in patients with diabetes and those with diabetic kidney disease. (C) A volcano plot illustrated the significant differences in plasma proteins between diabetic patients and those with DKD. (D) An analysis of protein–protein interactions highlighted significant differences in plasma proteins among patients with diabetes and diabetic kidney disease. (E) The analysis focused on plasma-specific proteins and their interactions in patients with DKD. (F, G) Investigated the enrichment of plasma-specific protein Gene Ontology (GO) and KEGG database pathways in patients with diabetic kidney disease. (H) The plasma levels of IGFBP2 and IGFBP4 in normal adults, diabetic patients, and diabetic kidney patients were quantified using Western blotting (WB). Data are presented as mean \pm SD ($n = 3$). $**p < .01$.



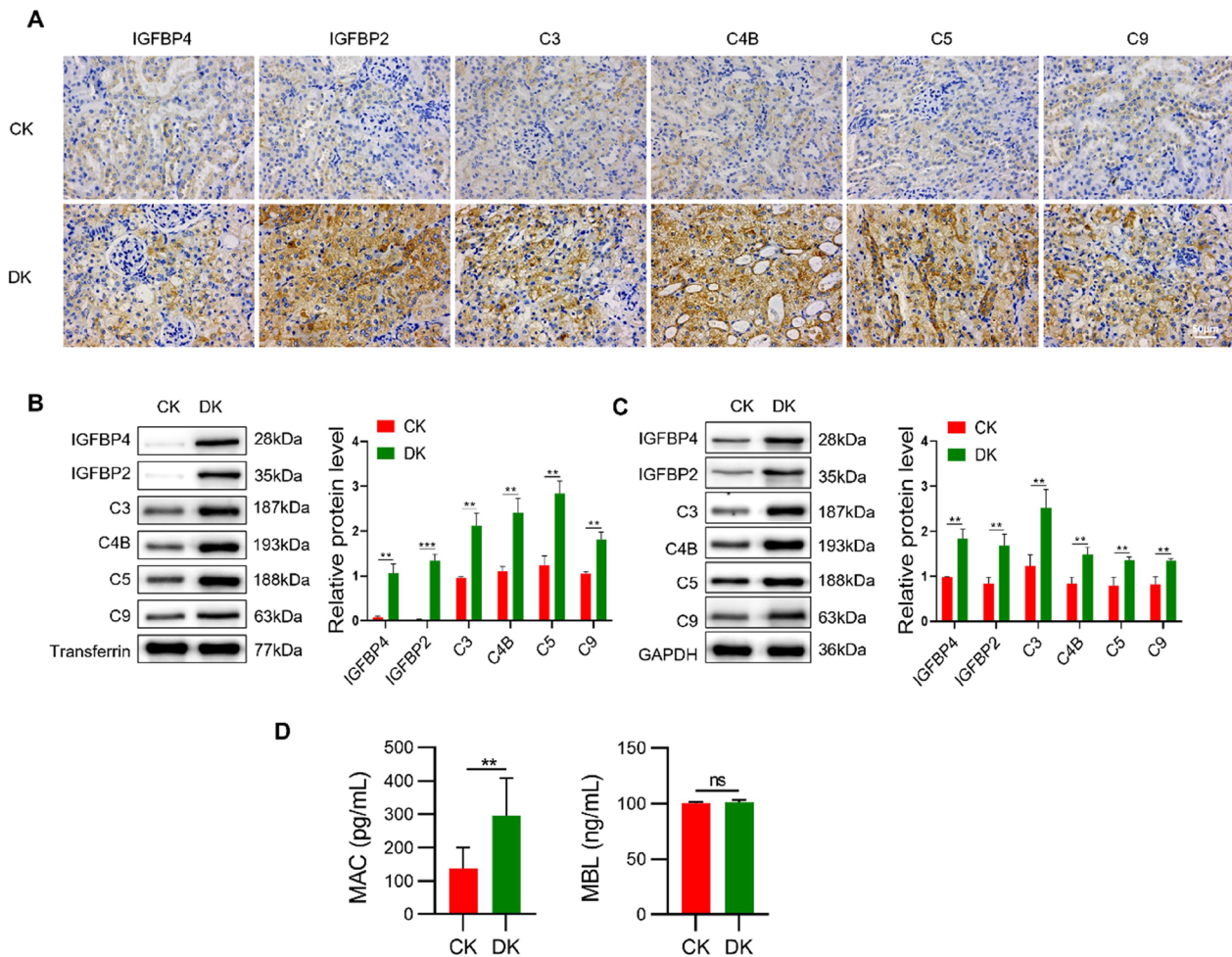


Figure 3. The effects of IGFBP2 and IGFBP4 on the complement pathway in DKD mice were examined. (A) The alterations in IGFBP2, IGFBP4, and complement proteins C3, C4B, C5, and C9 in the renal tissues of both normal and DKD mice were assessed using immunohistochemistry, with a scale bar of 50 μ m. (B) The levels of plasma IGFBP2, IGFBP4, and complement proteins C3, C4B, C5, and C9 in normal and DKD mice were analyzed via Western blotting (WB). (C) The changes in IGFBP2, IGFBP4, and complement proteins C3, C4B, C5, and C9 in the renal tissues of normal and DKD mice were also evaluated using WB. (D) Plasma levels of MAC and MBL were measured using ELISA in both normal and DKD mice. Data are presented as mean \pm SD, with $n = 3$. Statistical significance is indicated as $**p < .01$ and $***p < .001$.

to observe their functional alterations (Figure 5(A)). The levels of IGFBP2 and IGFBP4 secreted by HK-2 cells were significantly elevated (Figure 5(B)). It was observed that the number of M1-type THP-1 cells significantly increased, while the number of M2-type THP-1 cells significantly decreased (Figure 5(C)). Additionally, the expression levels of complement proteins C3, C4B, C5, and C9 in THP-1 cells were significantly elevated (Figure 5(D)), and the level of MAC was also significantly increased, whereas the level of MBL remained unchanged (Figure 5(E)). Further investigation into the interactions between macrophages and primary human renal podocytes revealed that the survival rate, apoptosis rate, and ROS content of primary human renal podocytes stimulated solely by high glucose and DKD mouse serum did not exhibit significant changes. However, when cultured with THP-1 cell supernatant, the survival rate of primary human renal podocytes significantly decreased, while the apoptosis rate significantly increased, along with a notable rise in ROS content (Figure 5(F–H)).

THP-1 cells IGFBP2/IGFBP4 activate the complement pathway to induce podocyte apoptosis

To further elucidate the mechanism of action of IGFBP2 and IGFBP4 (Figure 6(A)), we administered varying concentrations of recombinant IGFBP2 and IGFBP4 proteins to THP-1 cells to identify the optimal concentration for complement pathway activation. The results indicated that the levels of complement proteins C3, C4B, C5, C9, and MAC, all of which are products activated by the complement pathway, were significantly elevated following stimulation with recombinant IGFBP2 and IGFBP4 at concentrations of 50, 100, 200, and 400 ng/mL. In contrast, the levels of MBL remained unchanged (Figure 6(B)). The most pronounced activation of the complement pathway occurred at a concentration of 400 ng/mL for both IGFBP2 and IGFBP4; thus, this concentration was selected for subsequent experiments, both individually and in combination. Following stimulation of THP-1 cells with IGFBP2 and IGFBP4, whether alone or in combination, the levels of complement proteins C3, C4B, C5, C9, and MAC

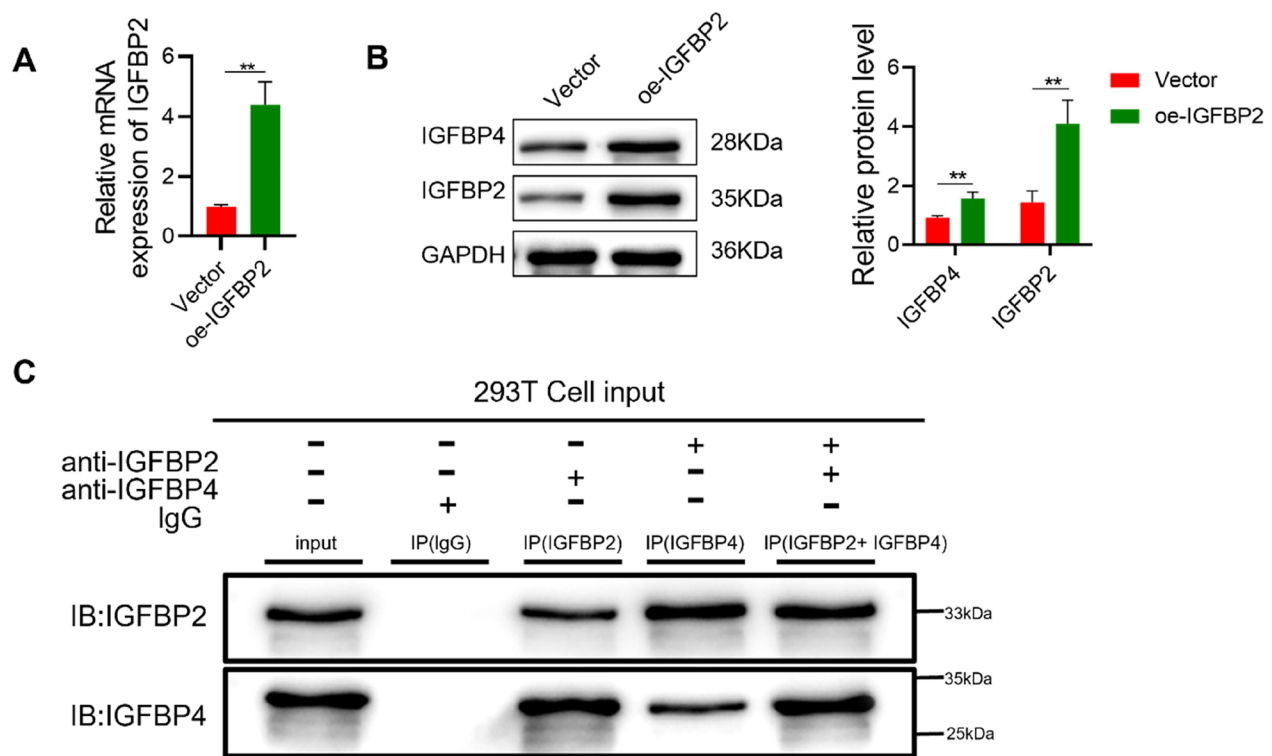


Figure 4. There is a protein interaction between IGFBP2 and IGFBP4. (A) IGFBP2 was overexpressed in 293T cells, and the expression level of IGFBP2 was assessed using qPCR to confirm the successful construction of the model. The group with overexpressed IGFBP2 is referred to as oe-IGFBP2. (B) Western blotting (WB) was employed to measure the levels of IGFBP2 and IGFBP4 following the overexpression of IGFBP2 in 293T cells. (C) Co-immunoprecipitation (Co-IP) was utilized to detect the formation of the IGFBP2 and IGFBP4 complex. Data are presented as mean \pm SD, with $n = 3$ and $**p < .01$.

were significantly elevated, while MBL levels did not exhibit significant changes (Figure 6(C)). Additionally, there was a notable increase in the number of M1-type THP-1 cells, whereas M2-type THP-1 cells were significantly reduced (Figure 6(D)). The supernatant from THP-1 cells cultured with IGFBP2 and IGFBP4 was subsequently collected to prepare culture medium for primary human renal podocytes. The survival rate of primary human renal podocytes cultured in THP-1 cell supernatants was significantly reduced. In contrast, stimulation with IGFBP2 protein and IGFBP4 protein, either alone or in combination, did not affect the survival rate (Figure 6(E)). Furthermore, the apoptosis rate of primary human renal podocytes cultured in THP-1 cell supernatants was significantly increased, while stimulation with IGFBP2 protein and IGFBP4 protein, both individually and in combination, had no impact on the apoptosis rate (Figure 6(F)). The ROS content in primary human renal podocytes cultured with THP-1 cell supernatant was elevated, whereas the ROS levels remained unchanged following stimulation with IGFBP2 protein and IGFBP4 protein, either alone or together (Figure 6(G)). Additionally, primary human renal podocytes cultured in THP-1 cell supernatant exhibited reduced cell-to-cell contacts, shrunken cell bodies, elongated or absent foot processes, and alterations in normal cell morphology. However, following stimulation with IGFBP2 protein and IGFBP4 protein, either alone or in combination, the podocytes appeared interlaced, tightly connected, and exhibited plump cell bodies (Figure 6(H)).

Discussion

Based on the report by the International Diabetes Federation in 2021, the global prevalence of diabetes was reported at 9% in 2019, leading to an estimated 463 million adults diagnosed with the condition. By 2021, this number had risen to 537 million, with predictions indicating a potential increase to 783 million by the year 2045 [11]. DKD is a major complication associated with diabetes, impacting nearly 30% of individuals with type 1 diabetes and 40% of those with type 2 diabetes [12]. As the number of people living with diabetes continues to grow globally, the incidence of DKD also increases. In developed countries, DKD contributes to 44.5% of the causes of end-stage renal disease (ESRD). Once individuals reach the ESRD stage, they usually require either dialysis or a kidney transplant for effective treatment. Nevertheless, due to a lack of available kidneys and the significant decline in life quality often tied to dialysis, many patients do not receive adequate care [13]. Furthermore, a considerable proportion of DKD patients may die prior to reaching the point where long-term dialysis or transplantation becomes necessary [12]. As a result, there is an urgent requirement to delve deeper into the molecular mechanisms that drive DKD and to uncover potential treatment options. Our research has identified 29 proteins present in patients with DKD, together with 68 co-expressed proteins, of which eight displayed significantly altered levels compared to the control group. Analysis of protein interaction networks

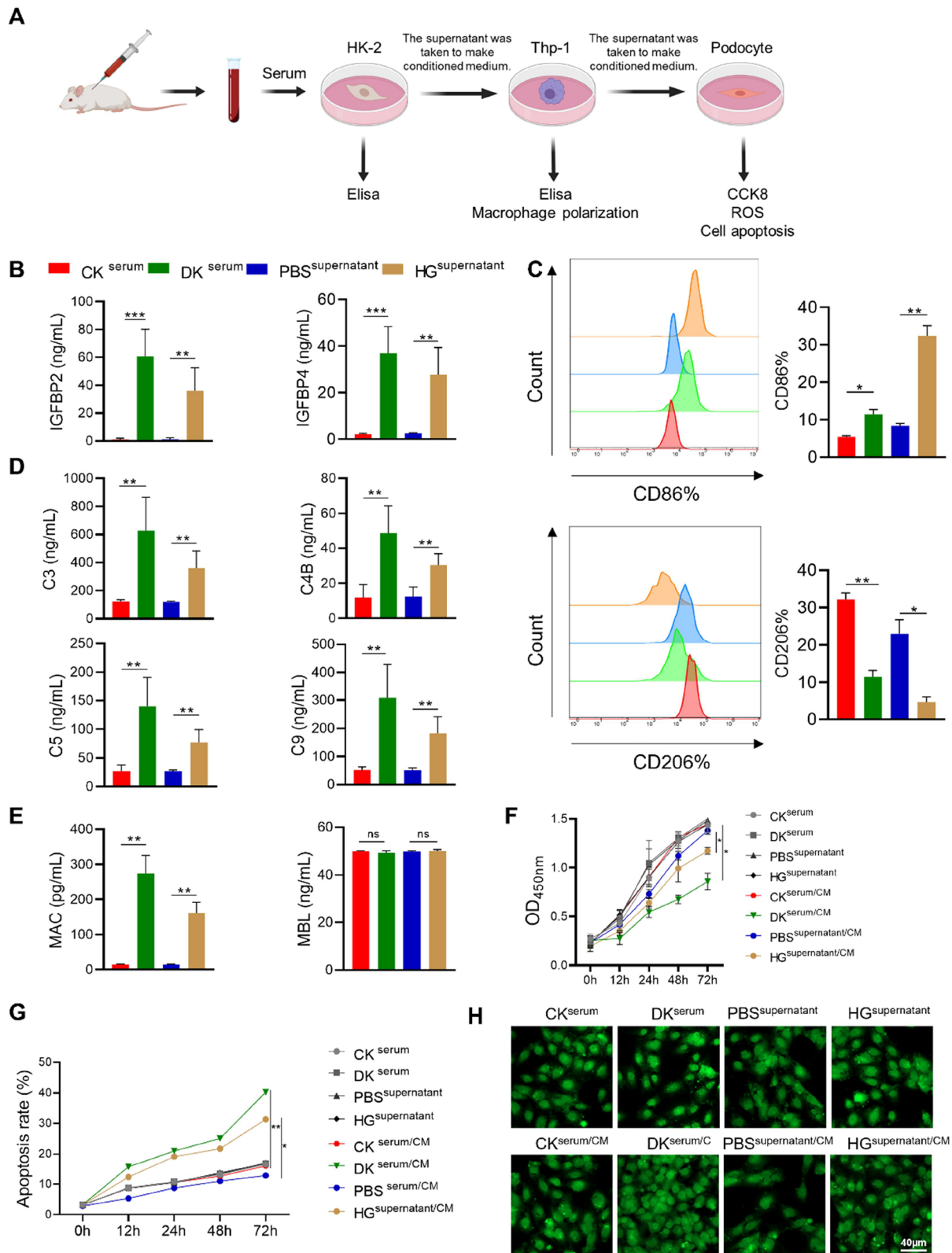


Figure 5. The crosstalk effect among HK-2 cells, THP-1 cells, and primary human renal podocytes was investigated as follows: (A) the serum from DKD mice (10%) was added to HK-2 cells for culture for 24h, after which relevant indicators were detected. The supernatant from HK-2 cells was then transferred to THP-1 cells to assess the functional changes in THP-1 cells, and subsequently, the THP-1 cell supernatant was added to primary human renal podocytes to observe their functional alterations. (B) The levels of IGFBP2 and IGFBP4 following HK-2 cell stimulation were measured. (C) The polarization of THP-1 cells was assessed using flow cytometry, where CD86% served as the marker for M1 polarization and CD206% indicated M2 polarization. (D) ELISA was employed to detect changes in complement proteins C3, C4B, C5, and C9 in THP-1 cells. (E) The levels of MAC and MBL in THP-1 cells were also measured using ELISA. (F) Podocyte proliferation was evaluated using the CCK-8 assay. (G) Apoptosis of primary human renal podocytes was analyzed through flow cytometry. (H) The expression of reactive oxygen species (ROS) in primary human renal podocytes was visualized by immunofluorescence, with green fluorescence indicating the intensity of ROS expression. Data are presented as mean \pm SD ($n = 3$; * $p < .05$, ** $p < .01$, *** $p < .001$).

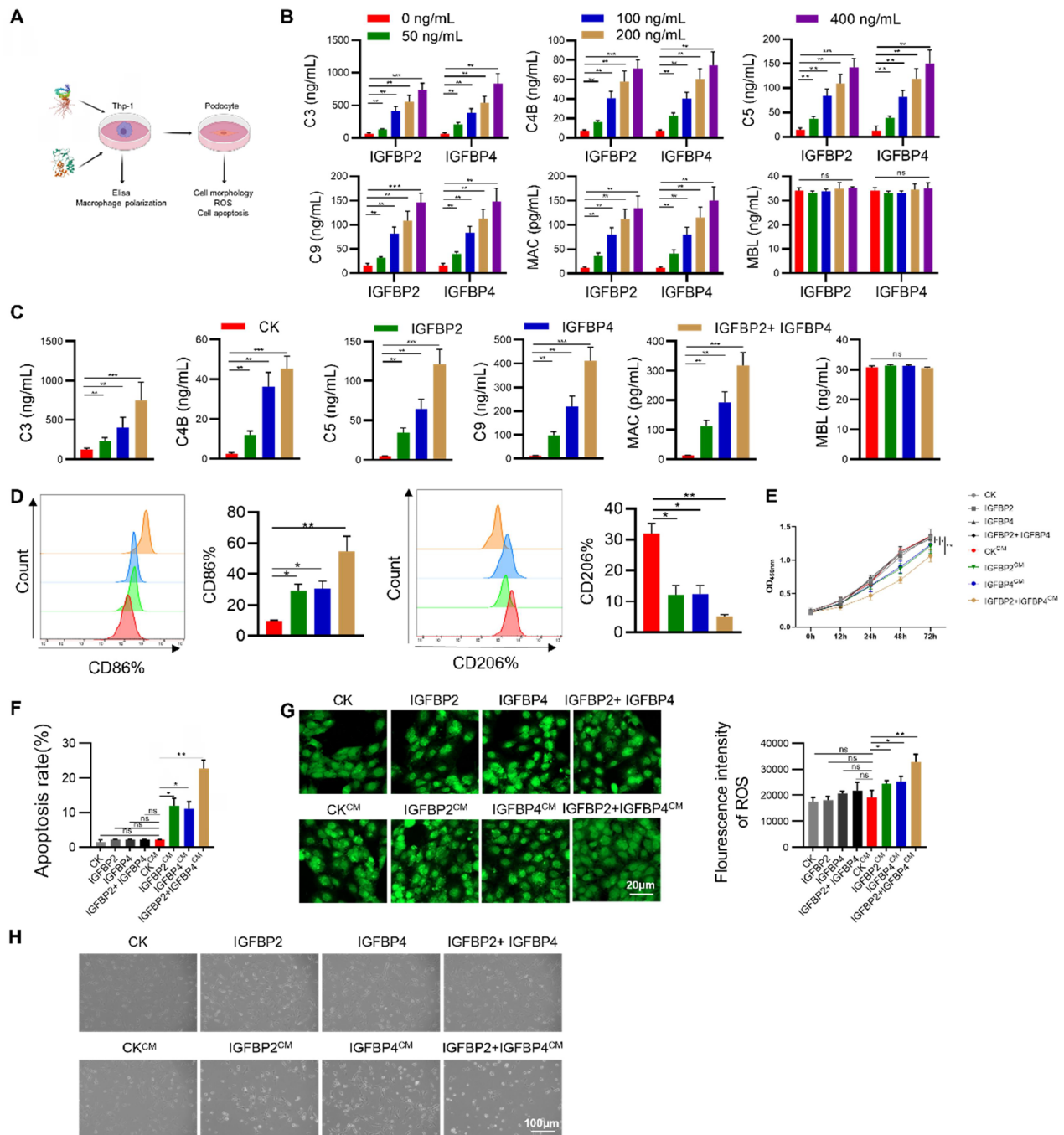


Figure 6. Effects of exogenous addition of IGFBP2 and IGFBP4 on THP-1 cells and primary human renal podocytes. (A) Following the addition of recombinant IGFBP2 and IGFBP4 proteins to THP-1 cells, the supernatant was collected for the assessment of related indices, which were subsequently applied to primary human renal podocytes to observe functional changes. (B) Different concentrations of recombinant IGFBP2 and IGFBP4 (50 ng/mL, 100 ng/mL, 200 ng/mL, and 400 ng/mL) were found to stimulate the levels of complement proteins C3, C4B, C5, C9, as well as MAC and MBL in THP-1 cells. (C) The effects of individually adding IGFBP2h or IGFBP4 recombinant protein, or their combined addition, on the levels of complement proteins C3, C4B, C5, C9, MAC, and MBL in THP-1 cells were assessed. (D) Flow cytometry analysis was conducted to determine the impact of IGFBP2h or IGFBP4 recombinant protein, either alone or in combination, on the polarization of THP-1 cells. (E) The influence of THP-1 cell supernatant on podocyte proliferation was evaluated using the CCK-8 assay. (F) The effect of THP-1 cell supernatant on podocyte apoptosis was measured through flow cytometry. (G) Immunofluorescence was utilized to observe the effect of THP-1 cell supernatant on ROS expression in primary human renal podocytes. (H) The impact of THP-1 cell supernatant on podocyte morphology was also assessed. Data are presented as mean \pm SD. $n = 3$; * $p < .05$, ** $p < .01$, *** $p < .001$.

indicated the presence of interactions between IGFBP2 and IGFBP4 within the specific proteins related to the DKD cohort, hinting at a possible link to the complement pathway.

Research shows a connection between IGFBPs and kidney development [14], acute kidney injury [15], and primary

kidney disorders such as IgAN [16]. Additionally, secondary kidney diseases, including DKD [17] and LN [18], are also associated with these proteins. Notably, it has been observed that levels of IGFBP2 significantly rise in response to diabetes and elevated glucose conditions. Furthermore, reducing

IGFBP2 expression can alleviate urinary protein excretion caused by STZ, diminish renal pathological damage, and curb glomerular hypertrophy in mouse models of DKD, while increased IGFBP2 expression has been linked to podocyte apoptosis [19]. Elevated IGFBP4 levels in cases of chronic renal failure are related to growth suppression and renal bone disease [20]. Our developed mouse model of DKD confirmed that the plasma expression levels of IGFBP2 and IGFBP4 in these diabetic mice positively correlate with fasting blood glucose and serum creatinine, while showing a negative correlation with serum albumin. This implies that higher expression of IGFBP2 and IGFBP4 might worsen kidney injury and promote the advancement of DKD, indicating a potential role of these proteins as therapeutic targets for this disease. Moreover, the secretion of IGFBP2 and IGFBP4 from HK-2 cells was significantly increased when these cells were exposed to injury in the serum of mice suffering from high glucose and DKD. Nonetheless, definitive research exploring the possible interactions between IGFBP2 and IGFBP4 in DKD is currently lacking. Our investigation, employing protein interaction assays, has identified for the first time a protein interaction between IGFBP2 and IGFBP4, suggesting their potential synergistic role in the progression of DKD.

The complement pathway becomes activated, resulting in the release of pro-inflammatory signals that promote vasodilation, and the release of cytokines and chemokines, as well as the chemical recruitment of neutrophils and macrophages. Such activation subsequently leads to the stimulation of macrophages, along with the enhancement, proliferation, and longevity of T cells and antigen-presenting cells [21]. Research, including both complement deposition studies and clinical findings, shows that the presence of complement component 1q (C1q) and complement component 3c (C3c), as observed through renal immunohistochemistry, correlates with more severe kidney damage in cases of DKD [22]. In a prolonged diabetic rat model, blocking C5 led to decreased urinary protein levels and less mesangial dilation [23]. Likewise, in db/db mice, the limitation of C5a was found to improve renal performance, lower tubulointerstitial fibrosis, and reduce lipid buildup in the kidneys. Additionally, antagonists for C5a and C3a receptors have been demonstrated to promote endothelium-to-myoblast transformation (EndMT) and reduce glomerular sclerosis in STZ-induced diabetic rat kidneys, as well as in human glomerular endothelial cells cultured in high glucose environments [24]. Despite these observations, the underlying mechanisms that activate the complement pathway in DKD are still insufficiently understood. Our findings reveal that the levels of IGFBP2 and IGFBP4 proteins in the plasma and renal tissues of DKD mice are significantly elevated, accompanied by a marked increase in the expression of complement proteins. This implies that IGFBP2 and IGFBP4 might be involved in the activation of the complement pathway in DKD.

The complement pathway serves as a key component of the immune response and plays a significant role in the development of kidney disease. Studies have shown that the polarization of M2 and M1 macrophages mediated by

complements may be involved in the formation of crescents seen in LN [25]. On the other hand, research suggests that glomeruli are especially susceptible to harm from circulating complement components, while local synthesis of complement, particularly through C3, often leads to tubular injury [26]. It is essential to activate immune cells and protect innate kidney cells for effective management of DKD; however, the relationship between these two processes demands more exploration. Podocytes, crucial for maintaining the glomerular filtration barrier, are linked to the pathogenesis of DKD, as the apoptosis of podocytes is a contributing factor [27]. These cells play a critical role in maintaining the structural and functional integrity of the glomeruli, and thus, apoptosis or a reduction in podocyte numbers can jeopardize the glomerular filtration membrane's integrity, leading to proteinuria often associated with glomerular diseases [27]. Our investigation demonstrated a marked rise in M1-type cells along with a significant decline in M2-type cells, correlated with the activation of the complement pathway in THP-1 cells after injury. Further experiments, which involved culturing primary human renal podocytes with the supernatant derived from THP-1 cells, revealed that podocyte proliferation was suppressed while apoptosis rates increased. This indicates that immune cells may have a regulatory effect on the innate kidney cells. In the initial stages of this study, we discovered that IGFBP2 and IGFBP4 can stimulate the complement pathway; however, their exact functions in the activation of the complement system and the interaction between macrophages and podocytes necessitate additional research. Interestingly, our results showed that the survival rate, as well as the content of ROS and apoptosis rate of primary human renal podocytes subjected solely to high glucose and serum from DKD mouse models, remained stable. Conversely, primary human renal podocytes cultured with supernatant from injured THP-1 cells experienced a significant reduction in survival rate and a pronounced increase in apoptosis, along with heightened ROS levels. Additionally, we obtained supernatant from THP-1 cells treated with IGFBP2 and IGFBP4 proteins to formulate a culture medium for primary human renal podocytes. The outcomes indicated that the growth and morphology of podocytes directly exposed to IGFBP2 and IGFBP4 proteins did not change. However, primary human renal podocytes grown in the presence of THP-1 cell supernatant showed a considerable drop in survival rate and an uptick in apoptosis, together with morphological alterations and increased ROS levels. These observations imply that IGFBP2 and IGFBP4, secreted by macrophages, may contribute to ROS buildup and promote apoptosis in podocytes.

The complement cascade can be triggered through three main pathways: the classical pathway, the MBL pathway, and the bypass pathway. Activation of the classical pathway occurs when immune complexes, including IgG and IgM, bind to C1q. In contrast, the MBL pathway becomes activated by carbohydrates on microbial cell surfaces and is mediated by MBL or other pattern recognition receptors [28]. We found that the levels of MAC, a co-product of complement

pathway activation, were significantly increased in both *in vivo* and *in vitro* experiments. However, the levels of MBL in the MBL pathway did not change significantly, suggesting that the MBL pathway is not involved in the development of DKD in our DKD mouse model.

Conclusions

We demonstrated that IGFBP2 and IGFBP4 interact to induce podocyte apoptosis through the activation of the macrophage complement pathway, thereby promoting the progression of DKD. Consequently, strategies aimed at inhibiting the levels of IGFBP2 and IGFBP4 in DKD may offer protective benefits for the kidneys.

Ethical approval

This study protocol of experiments on humans was reviewed and approved by Ethics Committees of Dongkeng Hospital. All methods were carried out in accordance with relevant guidelines and regulations. In addition, the study protocol of animal experiments was reviewed and approved by the IACUC of Ruige Biotechnology, approval number (20240508-002) and the animal experiments were performed in the accordance with ARRIVE guidelines (<https://arriveguidelines.org>).

Consent form

Verbal informed consent was obtained from all subjects and was in line with local guidelines.

Author contributions

Jieling Liang and Junfa Xu designed, performed the experiments, and wrote and revised the paper. Yangxiao Huang and Daping Peng performed *in vitro* experiments. Yali Xie and Yifei Liu reviewed and revised the paper. Xiuxia Lu and Yangxiao Huang designed the study and revised the paper. All authors contributed to analyze the results and approved the paper.

Disclosure statement

No potential conflict of interest was reported by the author(s).

Funding

This work was supported by Key Projects of Social Development Science and Technology in Dongguan in 2023 (Grant Number 20231800940302).

Data availability statement

The data that support the findings of this study are not publicly available due to their containing information that could compromise the privacy of research participants, but are available from the corresponding author J.f.X.

References

- [1] Expert Group of Chinese Society of Nephrology. Chinese guidelines for diagnosis and treatment of diabetic kidney disease. *Chin J Nephrol.* 2021;37(3):255–304.
- [2] Baxter RC. IGF binding proteins in cancer: mechanistic and clinical insights. *Nat Rev Cancer.* 2014;14(5):329–341.
- [3] Narayanan RP, Fu B, Heald AH, et al. IGFBP2 is a biomarker for predicting longitudinal deterioration in renal function in type 2 diabetes. *Endocr Connect.* 2013;1(2):95–102.
- [4] Bach L. Insulin-like growth factor binding proteins 4–6. *Best Pract Res Clin Endocrinol Metab.* 2015;29(5):713–722. doi: [10.1016/j.beem.2015.06.002](https://doi.org/10.1016/j.beem.2015.06.002).
- [5] Zhou R, Diehl D, Hoefflich A, et al. IGF-binding protein-4: biochemical characteristics and functional consequences. *J Endocrinol.* 2003;178(2):177–193. doi: [10.1677/joe.0.1780177](https://doi.org/10.1677/joe.0.1780177).
- [6] AlMajed HT, Abu-Farha M, Alshawaf E, et al. Increased levels of circulating IGFBP4 and ANGPTL8 with a prospective role in diabetic nephropathy. *Int J Mol Sci.* 2023;24(18):14244. doi: [10.3390/ijms241814244](https://doi.org/10.3390/ijms241814244).
- [7] Merle NS, Church SE, Fremeaux-Bacchi V, et al. Complement system. Part I – molecular mechanisms of activation and regulation. *Front Immunol.* 2015;6:262.
- [8] Merle NS, Leon J, Poillierat V, et al. Circulating FH protects kidneys from tubular injury during systemic hemolysis. *Front Immunol.* 2020;11:1772.
- [9] Tang SCW, Yiu WH. Innate immunity in diabetic kidney disease. *Nat Rev Nephrol.* 2020;16(4):206–222.
- [10] Sircar M, Rosales IA, Selig MK, et al. Complement 7 is up-regulated in human early diabetic kidney disease. *Am J Pathol.* 2018;188(10):2147–2154.
- [11] Sun H, Saeedi P, Karuranga S, et al. IDF Diabetes Atlas: global, regional and country-level diabetes prevalence estimates for 2021 and projections for 2045. *Diabetes Res Clin Pract.* 2022;183:109119. doi: [10.1016/j.diabres.2021.109119](https://doi.org/10.1016/j.diabres.2021.109119).
- [12] Tuttle K, Cherney D. Therapeutic transformation for diabetic kidney disease. *Kidney Int.* 2021;99(2):301–303. doi: [10.1016/j.kint.2020.10.003](https://doi.org/10.1016/j.kint.2020.10.003).
- [13] Collins AJ, Foley RN, Herzog C, et al. US renal data system 2010 annual data report. *Am J Kidney Dis.* 2011;57(1 Suppl. 1):A8, e1–e526. doi: [10.1053/j.ajkd.2010.10.007](https://doi.org/10.1053/j.ajkd.2010.10.007).
- [14] Wang S, Chi K, Wu D, et al. Insulin-like growth factor binding proteins in kidney disease. *Front Pharmacol.* 2022;12:807119.
- [15] Yu J-T, Hu X-W, Yang Q, et al. Insulin-like growth factor binding protein 7 promotes acute kidney injury by alleviating poly ADP ribose polymerase 1 degradation. *Kidney Int.* 2022;102(4):828–844.
- [16] Neuhaus J, Bauer F, Fitzner C, et al. Urinary biomarkers in the prediction of prognosis and treatment response in IgA nephropathy. *Kidney Blood Press Res.* 2018;43(5):1563–1572.
- [17] Song C, Wang S, Fu Z, et al. IGFBP5 promotes diabetic kidney disease progression by enhancing PFKFB3-mediated endothelial glycolysis. *Cell Death Dis.* 2022;13(4):340. doi: [10.1038/s41419-022-04803-y](https://doi.org/10.1038/s41419-022-04803-y).
- [18] Ding H, Kharboutli M, Saxena R, et al. Insulin-like growth factor binding protein-2 as a novel biomarker for disease activity and renal pathology changes in lupus nephritis. *Clin Exp Immunol.* 2015;184(1):11–18.

- [19] Wang X, Zhang Y, Chi K, et al. IGFBP2 induces podocyte apoptosis promoted by mitochondrial damage via integrin α 5/FAK in diabetic kidney disease. *Apoptosis*. 2024;29(7–8):1109–1125.
- [20] Ulinski T, Mohan S, Kiepe D, et al. Serum insulin-like growth factor binding protein (IGFBP)-4 and IGFBP-5 in children with chronic renal failure: relationship to growth and glomerular filtration rate. The European Study Group for Nutritional Treatment of Chronic Renal Failure in Childhood. German Study Group for Growth Hormone Treatment in Chronic Renal Failure. *Pediatr Nephrol*. 2000;14(7):589–597. doi: [10.1007/s004670000361](https://doi.org/10.1007/s004670000361).
- [21] Tan SM, Snelson M, Østergaard JA, et al. The complement pathway: new insights into immunometabolic signaling in diabetic kidney disease. *Antioxid Redox Signal*. 2022;37(10–12):781–801. doi: [10.1089/ars.2021.0125](https://doi.org/10.1089/ars.2021.0125).
- [22] Sun Z-J, Li X-Q, Chang D-Y, et al. Complement deposition on renal histopathology of patients with diabetic nephropathy. *Diabetes Metab*. 2018;45(4):363–368.
- [23] Fujita T, Ohi H, Komatsu K, et al. Complement activation accelerates glomerular injury in diabetic rats. *Nephron*. 1999;81(2):208–214.
- [24] Li L, Chen L, Zang J, et al. C3a and C5a receptor antagonists ameliorate endothelial–myofibroblast transition via the Wnt/ β -catenin signaling pathway in diabetic kidney disease. *Metabolism*. 2015;64(5):597–610. doi: [10.1016/j.metabol.2015.01.014](https://doi.org/10.1016/j.metabol.2015.01.014).
- [25] Tao J, Zhao J, Qi X-M, et al. Complement-mediated M2/M1 macrophage polarization may be involved in crescent formation in lupus nephritis. *Int Immunopharmacol*. 2021;101(Pt A):108278.
- [26] Sacks S, Zhou W. New boundaries for complement in renal disease. *J Am Soc Nephrol*. 2008;19(10):1865–1869. doi: [10.1681/ASN.2007101121](https://doi.org/10.1681/ASN.2007101121).
- [27] Vartak T, Godson C, Brennan E. Therapeutic potential of pro-resolving mediators in diabetic kidney disease. *Adv Drug Deliv Rev*. 2021;178:113965. doi: [10.1016/j.addr.2021.113965](https://doi.org/10.1016/j.addr.2021.113965).
- [28] Flyvbjerg A. The role of the complement system in diabetic nephropathy. *Nat Rev Nephrol*. 2017;13(5):311–318. doi: [10.1038/nrneph.2017.31](https://doi.org/10.1038/nrneph.2017.31).